Hindawi Publishing Corporation
EURASIP Journal on Wireless Communications and Networking
Volume 2008, Article ID 851726, 9 pages
doi:10.1155/2008/851726

Research Article

DOA Estimation in the Uplink of Multicarrier CDMA Systems

Antonio A. D'Amico, Michele Morelli, and Luca Sanguinetti

Department of Information Engineering, University of Pisa, Via Caruso, 56126 Pisa, Italy

Correspondence should be addressed to Antonio A. D'Amico, antonio.damico@iet.unipi.it

Received 15 May 2007; Accepted 23 October 2007

Recommended by Luc Vandendorpe

We consider the uplink of a multicarrier code-division multiple-access (MC-CDMA) network and assume that the base station is endowed with a uniform linear array. Transmission takes place over a multipath channel and the goal is the estimation of the directions of arrival (DOAs) of the signal from the active users. In a multiuser scenario, difficulties are primarily due to the large number of parameters involved in the estimation of the DOAs which makes this problem much more challenging than in single-user transmissions. The solution we propose allows estimating the DOAs of different users independently, thereby leading to a significant reduction in the system complexity. In the presence of multipath propagation, however, estimating the DOAs of a given user through maximum-likelihood methods remains a formidable task since it involves a search over a multidimensional domain. Therefore, we look for simpler solutions and discuss two alternative schemes based on the SAGE and ESPRIT algorithms.

1. INTRODUCTION

Antenna arrays at the base station (BS) can dramatically improve the capacity of a communication system [1–3]. Actually, they can be exploited in various ways. First, to form retrodirective beams that select the desired signals and attenuate the interfering ones. Secondly, antenna arrays make it possible to implement space-time selective transmission in the downlink. Finally, they can provide accurate localization of the user terminals [4], which is of interest in advanced handover schemes, public safety services, and intelligent transportation systems. In all these applications, accurate estimation of the directions of arrival (DOAs) of the desired signals is required.

DOA estimation has received much attention in the past years and several solutions are available in the technical literature (see [5–9] and the references therein). In particular, the schemes discussed in [5, 6] have good performance but are only devised for single-user applications and cannot be directly used in the uplink of a multiuser system. A tutorial review of subspace-based methods for DOA estimation is provided in [7]. The main drawback of these algorithms is that they can only handle a limited number of users since the overall number of resolvable paths cannot exceed the number of sensors in the antenna array. For this reason their application to a scenario with tens of users and several paths per user (as envisioned in fourth generation wireless systems) seems hardly viable. Schemes for estimating the DOAs in a CDMA multiuser system have been recently proposed in [8, 9]. In particular, the method discussed in [9] concentrates on a single user's parameters and models the multiple-access interference (MAI) as colored Gaussian noise. This idea is effective as it splits the multiuser DOA estimation problem into a series of simpler tasks in which DOAs of different users are estimated independently instead of jointly. A possible shortcoming of this method is that it requires knowledge of the MAI covariance matrix, which must be estimated in some manner.

In the present paper, we consider the uplink of a multicarrier code-division multiple-access (MC-CDMA) network [10, 11] and propose a method for estimating the DOAs of each active user. Transmission takes place over a multipath time-varying channel in which several paths with possibly different DOAs are present for each user. In a multiuser scenario the main obstacle is the large number of parameters involved in the estimation of the DOAs which makes this problem much more challenging than in single-user transmissions. A practical solution to this problem consists of separating each user from the others before applying conventional DOA estimation schemes. For this purpose, we first estimate

the channel response and the data symbols of each active user by resorting to the method discussed in [12]. Once channel estimates and data decisions are obtained, they are exploited to reconstruct the interfering signals, which are then subtracted from the received waveform. This produces an MAI-free signal which is finally used for DOA estimation. In this way the DOAs are estimated independently for each user but, contrarily to [9], no knowledge of the MAI statistics is required.

In spite of the significant simplification achieved by means of users' separation, estimating the DOAs of a given user through ML methods is still difficult as it involves a numerical search over a multidimensional domain. To reduce the system complexity we investigate two alternative schemes. The first is based on the space-alternating generalized expectation-maximization (SAGE) algorithm [13], in which the DOAs of a given user are estimated sequentially instead of jointly. This reduces the original multidimensional problem to a sequence of one-dimensional searches. The second scheme exploits the ESPRIT (Estimation of Signal Parameters by Rotational Invariance Techniques) algorithm [14] and estimates the DOAs in closed form.

The main contribution of this paper is a method for estimating the DOAs of all active users in an MC-CDMA scenario characterized by multiple resolvable paths. As mentioned previously, the major difficulty comes from the need of separating each user from the others before his DOAs can be estimated. Notice that conventional DOA estimation algorithms cannot be employed in such a scenario unless users' separation has been successfully completed, since otherwise the number of sensors in the antenna array should be prohibitively high (on the order of the total number of resolvable paths). To the best of the authors' knowledge, a similar problem has previously been addressed only in [15]. In particular, the solution proposed in [15] is tailored for the rate 3/4 space-time block code introduced by Tarokh in [16] and assumes a static channel with a single DOA for each user. Unfortunately, its extension to a time-varying multipath channel with possibly multiple DOAs for each user does not seem straightforward. A second contribution is a comparison between two popular schemes, namely, the SAGE and ESPRIT algorithms, both in terms of estimation accuracy and system complexity.

The rest of the paper is organized as follows. Section 2 describes the signal model and introduces basic notation. In Section 3 we derive the methods for estimating the DOAs. Simulation results are discussed in Section 4 and some conclusions are offered in Section 5.

2. SIGNAL MODEL

2.1. MC-CDMA system

We consider the uplink of an MC-CDMA network employing N subcarriers for the transmission of $N_u < N$ data symbols. The N_u modulated subcarriers are located in the middle of the signal bandwidth and are divided into smaller groups of Q elements [17]. The remaining $N - N_u$ subcarriers at the edges of the spectrum are not used to limit the out-of-band radiation (virtual carriers). The BS is equipped with P antennas and employs the subcarriers of a given group to communicate with K users that are separated through orthogonal Walsh-Hadamard (WH) codes of length $Q \geq K$. Without loss of generality, we concentrate on a single group and assume that the Q subcarriers are uniformly spread over the signal bandwidth so as to exploit the channel frequency diversity. We denote $\{i_n; 1 \leq n \leq Q\}$ the subcarrier indices in the group, with $i_n = i_1 + (n-1)N_u/Q$.

The ith symbol $a_k(i)$ of the kth user is spread over Q chips using the code sequence $\mathbf{c}_k = [c_k(1)\ c_k(2) \cdots c_k(Q)]^T$, where $c_k(n) \in \{\pm 1/\sqrt{Q}\}$ and the notation $(\cdot)^T$ means transpose operation. The resulting vector $a_k(i)\mathbf{c}_k$ is then mapped onto Q subcarriers using an OFDM modulator. The channel is assumed static over an OFDM block (slow-fading) and an N_G-point cyclic prefix (longer than the channel impulse response) is inserted to avoid interference between adjacent blocks.

At the receiver side the incoming waveform is first filtered and then sampled with period $T_s = T_B/(N + N_G)$, where T_B is the block duration. Next, the cyclic prefix is removed and the remaining samples are passed to an N-point discrete Fourier transform (DFT) unit. We concentrate on the mth MC-CDMA block and denote $\mathbf{X}_p(m) = [X_p(m, i_1)\ X_p(m, i_2) \cdots X_p(m, i_Q)]^T$ the demodulator outputs at the pth antenna corresponding to the Q subcarriers of the considered group. Also, we assume a quasisynchronous system in which each user is time-aligned to the BS reference in a way similar to that discussed in [18]. In these circumstances we have

$$\mathbf{X}_p(m) = \sum_{k=1}^{K} a_k(m)\mathbf{u}_{p,k}(m) + \mathbf{w}_p(m), \quad p = 1, 2, \ldots, P, \tag{1}$$

where $\mathbf{u}_{p,k}(m)$ is a Q-dimensional vector with entries

$$u_{p,k}(m, n) = H_{p,k}(m, i_n)c_k(n), \quad 1 \leq n \leq Q, \tag{2}$$

and $H_{p,k}(m, i_n)$ is the kth user's channel frequency response over the i_nth subcarrier at the pth antenna. Also, $\mathbf{w}_p(m) = [w_p(m, i_1)\ w_p(m, i_2) \cdots w_p(m, i_Q)]^T$ is thermal noise, which is modeled as a Gaussian vector with zero mean and covariance matrix $\sigma^2\mathbf{I}_Q$ (we denote $\mathbf{I}_Q$ the identity matrix of order Q).

2.2. Channel model

We assume that the P receive antennas are arranged in a uniform linear array with interelement spacing δ. The signal transmitted by each user propagates through a multipath channel with L distinct paths. Thus, the kth baseband channel impulse response (CIR) at the pth antenna during the mth MC-CDMA block takes the form

$$h_{p,k}(m, t) = \sum_{\ell=1}^{L} \alpha_{\ell,k}(m)e^{j(p-1)\omega_{\ell,k}(m)}g(t - \tau_{\ell,k}(m)), \tag{3}$$

where $g(t)$ is the convolution between the impulse responses of the transmit and receive filters, $\tau_{\ell,k}(m)$ is the delay of the

ℓ-path and $\alpha_{\ell,k}(m)$ the corresponding complex amplitude. Finally, $\omega_{\ell,k}(m)$ is defined as

$$\omega_{\ell,k}(m) = \frac{2\pi}{\lambda}\delta \sin[\varphi_{\ell,k}(m)], \tag{4}$$

where λ is the free-space wavelength and $\varphi_{\ell,k}(m)$ is the DOA of the ℓ-path. From (4) we see that measuring $\omega_{\ell,k}(m)$ is equivalent to measuring $\varphi_{\ell,k}(m)$ since there is a one-to-one relation between these quantities provided that $\varphi_{\ell,k}(m)$ is limited within $\pm 90^\circ$ and $\delta \le \lambda/2$. In the following we assume that the path delays and DOAs do not change significantly with time, that is, we set $\tau_{\ell,k}(m) \approx \tau_{\ell,k}$ and $\varphi_{\ell,k}(m) \approx \varphi_{\ell,k}$. Vice versa, the path gains $\alpha_{\ell,k}(m)$ are modeled as independent Gaussian random processes with zero-mean and average power $\sigma_\ell^2 = E\{|\alpha_{\ell,k}(m)|^2\}$.

The channel frequency response $H_{p,k}(m, i_n)$ is computed as the Fourier transform of $h_{p,k}(m,t)$ at $f = i_n/T$ and reads

$$H_{p,k}(m,i_n) = G(i_n)\sum_{\ell=1}^{L}\alpha_{\ell,k}(m)e^{-j2\pi i_n\tau_{\ell,k}/T}e^{j(p-1)\omega_{\ell,k}}, \tag{5}$$

where $T = NT_s$ is the duration of the useful part of the MC-CDMA block and $G(i_n)$ is the frequency response of $g(t)$ at the i_nth subcarrier. In the sequel, we assume that the N_u modulated subcarriers are located within the flat region of $G(i_n)$. In these circumstances, $H_{p,k}(m, i_n)$ reduces to

$$H_{p,k}(m,i_n) = \sum_{\ell=1}^{L}\alpha_{\ell,k}(m)e^{-j2\pi i_n\tau_{\ell,k}/T}e^{j(p-1)\omega_{\ell,k}}, \tag{6}$$

where $G(i_n)$ has been set equal to unity without loss of generality.

Notice that our multiuser scenario assumes KL resolvable paths. In practice, KL may be so large to prevent the joint estimation of the DOAs of all active users. To overcome this obstacle, we propose to estimate the DOAs of each user separately. In doing so we first compute estimates of the channel responses and data symbols of all active users. Next we exploit these results to reconstruct the interfering signals and cancel them out from the DFT output, thereby isolating the signal of the desired user. The problem of channel estimation and data detection is accomplished using the method discussed in [12] which provides accurate results with limited complexity. For this purpose, we assume that the MC-CDMA blocks are organized in frames. As shown in Figure 1, each frame is composed by N_B data blocks preceded by N_T training blocks that are exploited to get initial estimates of $\mathbf{H}_{p,k}(m)$ (acquisition). Such estimates are then updated during the data section of the frame (tracking) by means of the least-mean-square (LMS) algorithm.

3. DOA ESTIMATION

In this section, we show how the channel estimates and data decisions are exploited to perform DOA estimation. To this end, we denote by $\{\hat{a}_k(m)\}$ the data decisions and by $\{\hat{H}_{p,k}(m,i_n)\}$ the estimates of the channel frequency responses. We begin by computing the following quantities during the mth received block:

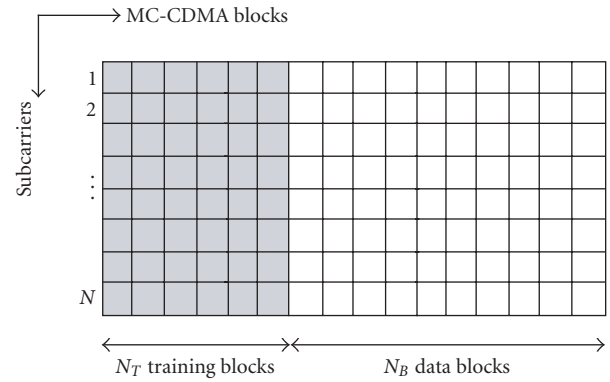

Figure 1: Frame structure.

$$y_{p,k}(m,i_n) = Q\hat{a}_k^*(m)c_k(n)\left[X_p(m,i_n) - \sum_{\substack{\ell=1\\ \ell\neq k}}^{K}\hat{a}_\ell(m)c_\ell(n)\hat{H}_{p,\ell}(m,i_n)\right], \quad k = 1,2,\ldots,K. \tag{7}$$

Substituting (1)-(2) into (7) and assuming $\hat{H}_{p,\ell}(m,i_n) \approx H_{p,\ell}(m,i_n)$ and $\hat{a}_\ell(m) \approx a_\ell(m)$ yields

$$y_{p,k}(m,i_n) = H_{p,k}(m,i_n) + w_p(m,i_n), \tag{8}$$

where we have set $|a_k(m)| = 1$ which is valid for PSK constellations. Letting $d_{\ell,k}(m,i_n) = \alpha_{\ell,k}(m)e^{-j2\pi i_n\tau_{\ell,k}/T}$, from (6) we see that $y_{p,k}(m,i_n)$ can also be written as

$$y_{p,k}(m,i_n) = \sum_{\ell=1}^{L}d_{\ell,k}(m,i_n)e^{j(p-1)\omega_{\ell,k}} + w_p(m,i_n). \tag{9}$$

It is worth noting that apart from thermal noise, only the contribution of the kth user is present in the right-hand side (RHS) of (9). This amounts to saying that the quantities $\{y_{p,k}(m,i_n)\}$ are MAI-free and, therefore, they can be used to estimate the DOAs of the kth user. In this way, DOA estimation is performed independently for each active user instead of jointly and the complexity of the overall estimation process is significantly reduced.

As mentioned in Section 2.2, measuring $\omega_{\ell,k}$ is equivalent to measuring the DOA $\varphi_{\ell,k}$. Without loss of generality, in this section we concentrate on the first user and aim at estimating $\boldsymbol{\omega}_1 = [\omega_{1,1}\ \omega_{2,1}\ \cdots\ \omega_{L,1}]^T$ based on the observation of $\{y_{p,1}(m,i_n)\}$. Since the ML estimation of $\boldsymbol{\omega}_1$ is prohibitively complex as it involves a numerical search over a multidimensional domain, in the sequel we discuss two practical DOA estimators based on the SAGE and ESPRIT algorithms. For notational simplicity, we drop the subscript identifier for the first user.

3.1. ML estimation

During the mth received block, the quantities $\{y_p(m, i_n)\}$ are arranged into P-dimensional vectors

$$\mathbf{y}(m, i_n) = [y_1(m, i_n)\ y_2(m, i_n) \cdots y_P(m, i_n)]^T \quad n = 1, 2, \ldots, Q. \tag{10}$$

We assume slow channel variations so that $d_\ell(m, i_n)$ can be considered practically constant over N_s consecutive blocks. Then, we divide the data section of the frame into adjacent segments, each containing N_s blocks, and compute the following average:

$$\mathbf{Y}_r(i_n) = \frac{1}{N_s} \sum_{i=0}^{N_s-1} \mathbf{y}(i + rN_s - N_s + N_T, i_n), \quad r = 1, 2, \ldots, R, \tag{11}$$

where r is the segment index and R denotes the number of segments within the frame (the number of data blocks in each frame is $N_B = N_s \times R$). Substituting (9) into (11), bearing in mind that $d_\ell(m, i_n) \approx d_\ell(rN_s - N_s/2, i_n)$ over the rth segment (i.e., for $N_T + rN_s - N_s \le m \le N_T + rN_s - 1$), yields

$$\mathbf{Y}_r(i_n) = \sum_{\ell=1}^{L} d_{\ell,r}(i_n)\mathbf{f}(\omega_\ell) + \boldsymbol{\eta}_r(i_n), \tag{12}$$

where $d_{\ell,r}(i_n) = d_\ell(rN_s - N_s/2, i_n)$, $\mathbf{f}(\omega_\ell)$ has entries $[\mathbf{f}(\omega_\ell)]_p = e^{j(p-1)\omega_\ell}$ $(1 \le p \le P)$ and $\{\boldsymbol{\eta}_r(i_n)\}$ are statistically independent Gaussian vectors with zero-mean and covariance matrix $\mathbf{C}_\eta = (\sigma^2/N_s)\mathbf{I}_P$. Letting $\mathbf{F}(\boldsymbol{\omega}) = [\mathbf{f}(\omega_1)\ \mathbf{f}(\omega_2) \cdots \mathbf{f}(\omega_L)]$, we may rewrite (12) in the equivalent form

$$\mathbf{Y}_r(i_n) = \mathbf{F}(\boldsymbol{\omega})\mathbf{d}_r(i_n) + \boldsymbol{\eta}_r(i_n), \tag{13}$$

where $\mathbf{d}_r(i_n)$ has entries $[\mathbf{d}_r(i_n)]_\ell = d_{\ell,r}(i_n)$ for $1 \le \ell \le L$.

We now jointly estimate $\boldsymbol{\omega}$ and $\{\mathbf{d}_r(i_n)\}$ based on the observation of $\{\mathbf{Y}_r(i_n)\}$ for $1 \le r \le R$ and $1 \le n \le Q$. Dropping irrelevant terms and factors, the log-likelihood function for $\boldsymbol{\omega}$ and $\{\mathbf{d}_r(i_n)\}$ takes the form

$$\Lambda(\{\tilde{\mathbf{d}}_r(i_n)\}, \tilde{\boldsymbol{\omega}}) = -\sum_{r=1}^{R}\sum_{n=1}^{Q} \left\| \mathbf{Y}_r(i_n) - \mathbf{F}(\tilde{\boldsymbol{\omega}})\tilde{\mathbf{d}}_r(i_n) \right\|^2, \tag{14}$$

where $\{\tilde{\mathbf{d}}_r(i_n)\}$ and $\tilde{\boldsymbol{\omega}}$ are trial values of the unknown parameters while $\|\cdot\|$ denotes Euclidean norm. Keeping $\tilde{\boldsymbol{\omega}}$ fixed and letting $\tilde{\mathbf{d}}_r(i_n)$ vary, the minimum of (14) is achieved for

$$\hat{\mathbf{d}}_r(i_n) = [\mathbf{F}^H(\tilde{\boldsymbol{\omega}})\mathbf{F}(\tilde{\boldsymbol{\omega}})]^{-1}\mathbf{F}^H(\tilde{\boldsymbol{\omega}})\mathbf{Y}_r(i_n), \quad 1 \le r \le R,\ 1 \le n \le Q. \tag{15}$$

Next, substituting (15) into (14) and maximizing with respect to $\tilde{\boldsymbol{\omega}}$ produce

$$\hat{\boldsymbol{\omega}} = \arg\max_{\tilde{\boldsymbol{\omega}}} \left\{ \sum_{r=1}^{R}\sum_{n=1}^{Q} \mathbf{Y}_r^H(i_n)\mathbf{F}(\tilde{\boldsymbol{\omega}}) \times [\mathbf{F}^H(\tilde{\boldsymbol{\omega}})\mathbf{F}(\tilde{\boldsymbol{\omega}})]^{-1}\mathbf{F}^H(\tilde{\boldsymbol{\omega}})\mathbf{Y}_r(i_n) \right\}. \tag{16}$$

Unfortunately there is no closed form solution to the maximization of (16). The only possible approach is to perform a search over the L-dimensional space spanned by $\tilde{\boldsymbol{\omega}}$. As the computational load would be too intense, in the next subsection we employ the SAGE algorithm to find an approximate solution of (16).

Remark 1. The ML estimators (15)-(16) have been derived using channel estimates given in (7). In principle, one can directly use the estimates provided by the LMS channel tracker, which are more or less correlated depending on the value of the step-size employed in the tracking algorithm. In contrast, assuming perfect interference cancellation, it is easily recognized that (7) provides uncorrelated channel estimates that facilitate the derivation of the joint ML estimator of $\boldsymbol{\omega}$ and $\{\mathbf{d}_r(i_n)\}$. Since the additional complexity involved by (7) is negligible, we have adopted the latter approach.

3.2. SAGE-based estimation

In a variety of ML estimation problems the maximization of the likelihood function is analytically unfeasible as it involves a numerical search over a huge number of parameters. In these cases the SAGE algorithm proves to be effective as it achieves the same final result with a comparatively simpler iterative procedure. Compared with the more familiar EM algorithm [19], the SAGE has a faster convergence rate. The reason is that the maximizations involved in the EM algorithm are performed with respect to all the unknown parameters simultaneously, which results in a slow process that requires searches over spaces with many dimensions. Vice versa, the maximizations in SAGE are performed varying small groups of parameters at a time. In the following, the SAGE algorithm is applied to our problem without further explanation. The reader is referred to [13] for details.

Returning to the joint estimation of $\boldsymbol{\omega}$ and $\{\mathbf{d}_r(i_n)\}$, we apply the SAGE algorithm in such a way that the parameters of a single path are updated at a time. This leads to the following procedure consisting of cycles and steps. A cycle is made of L steps and each step updates the parameters of a single path. In particular, the ℓ-step of the ith cycle looks for the minimum of

$$\lambda(\{\tilde{d}_{\ell,r}(i_n)\}, \tilde{\omega}_\ell) = \sum_{r=1}^{R}\sum_{n=1}^{Q} \left\| \mathbf{Y}_{\ell,r}^{(i)}(i_n) - \tilde{d}_{\ell,r}(i_n)\mathbf{f}(\tilde{\omega}_\ell) \right\|^2, \tag{17}$$

where $\mathbf{Y}_{\ell,r}^{(i)}(i_n) \in \mathbb{C}^P$ is defined as

$$\mathbf{Y}_{\ell,r}^{(i)}(i_n) = \mathbf{Y}_r(i_n) - \sum_{q=1}^{\ell-1} \hat{d}_{q,r}^{(i)}(i_n)\mathbf{f}(\hat{\omega}_q^{(i)}) - \sum_{q=\ell+1}^{L} \hat{d}_{q,r}^{(i-1)}(i_n)\mathbf{f}(\hat{\omega}_q^{(i-1)}), \tag{18}$$

and $\{\hat{d}_{q,r}^{(i)}(i_n), \hat{\omega}_q^{(i)}\}$ denotes the estimate of $\{d_{q,r}(i_n), \omega_q\}$ at the ith cycle. It is worth noting that $\mathbf{Y}_{\ell,r}^{(i)}(i_n)$ represents an expurgated version of $\mathbf{Y}_r(i_n)$, in which the latest estimates of

$\{d_{q,r}(i_n), \omega_q\}$ are exploited to cancel out the multipath interference. Minimizing (17) with respect to $\{\widetilde{d}_{\ell,r}(i_n), \widetilde{\omega}_\ell\}$ produces

$$\hat{\omega}_\ell^{(i)} = \arg\max_{\widetilde{\omega}} \left\{\Psi_\ell^{(i)}(\widetilde{\omega})\right\}, \tag{19}$$

$$\hat{d}_{\ell,r}^{(i)}(i_n) = \frac{1}{P}\mathbf{f}^H(\hat{\omega}_\ell^{(i)})\mathbf{Y}_{\ell,r}^{(i)}(i_n), \quad 1 \le r \le R,\ 1 \le n \le Q, \tag{20}$$

with

$$\Psi_\ell^{(i)}(\widetilde{\omega}) = \sum_{r=1}^{R}\sum_{n=1}^{Q}\left|\mathbf{f}^H(\widetilde{\omega})\mathbf{Y}_{\ell,r}^{(i)}(i_n)\right|^2. \tag{21}$$

Note that only one-dimensional searches are involved in (19).

The following remarks are of interest.

(1) The maximization in the RHS of (19) is pursued through a two-step procedure. The first (*coarse search*) computes $\Psi_\ell^{(i)}(\widetilde{\omega})$ over a grid of N_g values, say $\{\widetilde{\omega}_\ell(j); j = 1, 2, \ldots, N_g\}$, and determines the location $\widetilde{\omega}_{\max}$ of the maximum. In the second step (*fine search*) the quantities $\{\Psi_\ell^{(i)}(\widetilde{\omega}_\ell(j))\}$ are interpolated and the local maximum nearest to $\widetilde{\omega}_{\max}$ is found.

(2) From (21) it follows that $\Psi_\ell^{(i)}(\widetilde{\omega})$ is a periodic function of $\widetilde{\omega}$ with period 2π. Thus, the maximum of $\Psi_\ell^{(i)}(\widetilde{\omega})$ lies in the interval $(-\pi, \pi]$ and, in consequence, the estimator (19) gives correct results provided that $|\omega_\ell| < \pi$. From (4) it is seen that this condition is easily met using an antenna array with interelement spacing less than half the free-space wavelength.

(3) In applying the SAGE we have implicitly assumed knowledge of the number L of paths. In practice L is unknown and must be established in some way. One possible way is to choose L large enough so that all the paths with significant energy are considered. Alternatively, an estimate of L can be obtained in the first cycle as follows. Physical reasons and simulation results indicate that in any cycle the multipath components are taken in a decreasing order of strength. On the other hand, if $\{\hat{d}_{\ell,r}^{(1)}(i_n)\}$ are the estimates of $\{d_{\ell,r}(i_n)\}$ at the first cycle, an indication of the energy of the ℓth path is

$$\hat{E}_\ell = \frac{1}{RQ}\sum_{r=1}^{R}\sum_{n=1}^{Q}\left|\hat{d}_{\ell,r}^{(1)}(i_n)\right|^2. \tag{22}$$

Thus, the first cycle may be stopped at that step, say ℓ', where $\hat{E}_{\ell'}$ drops below a prefixed threshold and $\hat{L} = \ell' - 1$ may be taken as an estimate of the number of significant paths.

(4) The computational load of the SAGE is assessed as follows. Evaluating $\{\mathbf{Y}_{\ell,r}^{(i)}(i_n)\}$ for $r = 1, 2, \ldots, R$ and $n = 1, 2, \ldots, Q$ needs $O(RQLP)$ operations at each step. The complexity involved in the computation of $\{\hat{d}_{\ell,r}^{(i)}(i_n)\}$ in (20) is $O(RQP)$ while $O(RQPN_g)$ operations are required to compute the quantities $\Psi_\ell^{(i)}(\widetilde{\omega}(j))$ for $j = 1, 2, \ldots, N_g$. Denoting N_i the number of cycles and bearing in mind that each cycle is made of L steps, it follows that the overall complexity of the SAGE is $O[RQLPN_i(L + N_g + 1)]$.

3.3. ESPRIT-based estimation

An alternative approach for estimating the DOAs relies on subspace-based methods like the MUSIC (Multiple Signal Classication) [20] or ESPRIT algorithms [14]. In the following we discuss DOA estimation based on ESPRIT. The reason is that this method provides estimates in closed form while a grid-search is needed with MUSIC.

To begin, we exploit vectors $\{\mathbf{y}(m, i_n)\}$ in (10) to compute the sample correlation matrix

$$\hat{\mathbf{R}}_y = \frac{1}{N_B Q}\sum_{n=1}^{Q}\sum_{m=N_T}^{N_T+N_B-1}\mathbf{y}(m, i_n)\mathbf{y}^H(m, i_n). \tag{23}$$

Then, based on the forward-backward (FB) approach [21], we obtain the following modified sample correlation matrix

$$\widetilde{\mathbf{R}}_y = \frac{1}{2}(\hat{\mathbf{R}}_y + \mathbf{J}\hat{\mathbf{R}}_y^T\mathbf{J}), \tag{24}$$

in which $\mathbf{J}$ is the exchange matrix with 1's on its antidiagonal and 0's elsewhere.

In the ESPRIT method, the eigenvectors associated with the L largest eigenvalues of $\widetilde{\mathbf{R}}_y$ are arranged into a $P \times L$ matrix $\mathbf{V} = [\mathbf{v}_1\ \mathbf{v}_2 \cdots \mathbf{v}_L]$. Next, we consider the matrices $\mathbf{V}_1 = [\mathbf{I}_{P-1}\ \mathbf{0}]\mathbf{V}$ and $\mathbf{V}_2 = [\mathbf{0}\ \mathbf{I}_{P-1}]\mathbf{V}$, where $\mathbf{0}$ is an L-dimensional column vector with zero entries. The estimate of ω_ℓ is eventually obtained as

$$\hat{\omega}_\ell = \arg\{\lambda_\ell^*\}, \quad \ell = 1, 2, \ldots, L, \tag{25}$$

where $\{\lambda_1, \lambda_2, \ldots, \lambda_L\}$ are the eigenvalues of

$$\mathbf{S} = (\mathbf{V}_1^H\mathbf{V}_1)^{-1}\mathbf{V}_1^H\mathbf{V}_2, \tag{26}$$

and $\arg\{\lambda_\ell^*\}$ denotes the phase angle of λ_ℓ^* in the interval $[-\pi, \pi)$.

The following remarks are of interest.

(1) A necessary condition for the existence of $(\mathbf{V}_1^H\mathbf{V}_1)^{-1}$ in RHS of (26) is that the number of rows in $\mathbf{V}_1$ is greater than or equal to the number of columns. Since $\mathbf{V}_1$ has dimension $(P-1) \times L$, the above condition implies that $P \ge L + 1$, that is, the number of antennas must be greater than the number of multipath components. We also observe that the inverse of $\mathbf{F}^H(\widetilde{\boldsymbol{\omega}})\mathbf{F}(\widetilde{\boldsymbol{\omega}})$ in the ML estimator (16) exists provided that $\mathbf{F}(\widetilde{\boldsymbol{\omega}})$ is full rank and $P \ge L$. Thus, DOA estimation with ESPRIT needs one more antenna compared with the ML estimator. It is worth noting that the minimum number of antennas required by both schemes is *independent* of the number K of contemporarily active users.

(2) The number of paths can be estimated using the minimum description length (MDL) criterion [22]. To this purpose, let $\mu_1 \ge \mu_2 \cdots \ge \mu_P$ be the eigenvalues of

the correlation matrix $\widetilde{\mathbf{R}}_y$ in (24) (arranged in a nonincreasing order of magnitude). Then, an estimate of L is computed as

$$\hat{L} = \arg \min_{\widetilde{L}\in\{0,1,\ldots,P-1\}} \left\{ -N_B Q(P-\widetilde{L}) \log\left[\frac{\mathrm{GM}(\widetilde{L})}{\mathrm{AM}(\widetilde{L})}\right] + \frac{1}{4}\widetilde{L}(2P-\widetilde{L}+1)\log(N_B Q)\right\}, \tag{27}$$

where $\widetilde{L}$ is a trial value of L while $\mathrm{GM}(\widetilde{L})$ and $\mathrm{AM}(\widetilde{L})$ denote the *geometric* and *arithmetic* means of $\{\mu_i; \widetilde{L}+1 \le i \le P\}$ respectively, that is,

$$\mathrm{GM}(\widetilde{L}) = \left[\prod_{i=\widetilde{L}+1}^{P} \mu_i\right]^{1/(P-\widetilde{L})}, \qquad \mathrm{AM}(\widetilde{L}) = \frac{1}{P-\widetilde{L}} \sum_{i=\widetilde{L}+1}^{P} \mu_i. \tag{28}$$

(3) The complexity of the ESPRIT is assessed as follows. Evaluating $\hat{\mathbf{R}}_y$ in (23) needs $O(P^2 N_B Q)$ operations. Bearing in mind that inverting an $L \times L$ matrix requires $O(L^3)$ operations, it follows that the complexity involved in the computation of $\mathbf{S}$ in (26) is approximately $O[L^2(L+3P)]$. Finally, computing the eigenvectors of $\mathbf{S}$ needs $O(L^3)$ operations. In summary, the overall complexity of the ESPRIT is $O[P^2 N_B Q + L^2(2L+3P)]$. In writing this figure we have ignored the operations required to compute $\widetilde{\mathbf{R}}_y$, $\mathbf{V}_1$, and $\mathbf{V}_2$ since these matrices are easily obtained from $\hat{\mathbf{R}}_y$ with negligible complexity.

4. SIMULATION RESULTS

4.1. System parameters

We consider a cellular system operating over a typical urban area with a cell radius of 1 km. The transmitted symbols belong to a QPSK constellation and are obtained from the information bits through a Gray map. The number of modulated subcarriers is $N_u = 48$ and the DFT has dimension $N = 64$. Walsh-Hadamard codes of length $Q = 8$ are used for spreading purposes. The signal bandwidth is $B = 8$ MHz, so that the useful part of each MC-CDMA block has length $T = N/B = 8$ microseconds. The sampling period is $T_s = T/N = 0.125$ microsecond and a cyclic prefix of $T_G = 2$ microseconds is adopted to eliminate interblock interference. This corresponds to an extended block (including the cyclic prefix) of 10 microseconds. The users are synchronous within the cyclic prefix and have the same power. The carrier frequency is $f_0 = 2$ GHz (corresponding to a wavelength $\lambda = 15$ cm) and the interelement spacing in the antenna array is $\delta = \lambda/2$. The channel impulse responses of the active users are generated as indicated in (3) with three paths ($L = 3$). Pulse $g(t)$ has a raised-cosine Fourier transform with roll-off 0.22 and duration $T_g = 8T_s = 1$ microsecond. The path delays and DOAs of the desired user are equal to ($\tau_1 = 0, \varphi_1 = 0^\circ$), ($\tau_2 = 1.5T_s$, $\varphi_2 = -20^\circ$), and ($\tau_3 = 3.5T_s$, $\varphi_3 = 45^\circ$). Vice versa, path delays and DOAs of the interfering users are uniformly distributed within [0, 1] microseconds and $[-60^\circ, 60^\circ]$, respectively, and are kept constant over a frame. For all active users (including the desired one), the path gains have powers

$$\sigma_\ell^2 = \sigma_H^2 \exp(-\ell), \quad \ell = 0, 1, 2, \tag{29}$$

where σ_H^2 is chosen such that the channel energy is normalized to unity, that is, $E\{\|\mathbf{H}_{p,k}(m)\|^2\} = 1$. Each path varies independently of the others within a frame and is generated by filtering a white Gaussian process in a third-order lowpass Butterworth filter. The 3-dB bandwidth of the filter is taken as a measure of the Doppler rate $f_D = f_0 v/c$, where v denotes the speed of the mobile terminal and $c = 3 \times 10^8$ m/s is the speed of light.

A simulation run begins with the generation of the channel responses of each user. Channel acquisition is performed using Walsh-Hadamard training sequences of length $N_T = 8$ while channel tracking is accomplished by exploiting data decisions provided by a parallel interference cancellation (PIC) receiver [12]. Throughout simulations the number of data blocks per frame is set to $N_B = 128$. Once channel estimates and data decisions are obtained, they are passed to the proposed SAGE- or ESPRIT-based DOA estimators. The SAGE computes the function $\Psi_\ell^{(i)}(\widetilde{\omega})$ over a grid of $N_g = 64$ values and it is stopped at the end of the second cycle ($N_i = 2$). Parameter N_s in (11) is fixed to 16, so that $R = N_B/N_s = 8$. The mobile velocity, the number of users, and the number of antennas are varied throughout simulations so as to assess their impact on the system performance.

4.2. Performance assessment

The system performance has been assessed in terms of root mean-square-error (RMSE) of the DOA estimates. For simplicity, the number L of paths is assumed perfectly known at the receiver.

Figure 2 illustrates the performance of the SAGE-based scheme versus E_b/N_0 (E_b is the average received energy per bit and $N_0/2$ is the two-sided noise power spectral density) for a half-loaded system ($K = 4$). The mobile speed is 10 m/s and the number of sensors in the array is $P = 6$. Marks indicate simulation results while solid lines are drawn to ease the reading. We see that the curves exhibit a floor. In particular, the RMSE of the weakest path is approximately 15 degrees for $E_b/N_0 > 10$ dB. The appearance of the floor can be explained as follows. Inspection of (19) and (21) reveals that at the first step of the first cycle, the SAGE looks for the maximum of the periodogram $\psi_1^{(1)}(\widetilde{\omega})$. Neglecting the effect of thermal noise, we expect that $\psi_1^{(1)}(\widetilde{\omega})$ has three peaks located at the angular frequencies $\omega_i = \pi \sin \varphi_i$ for $i = 1, 2, 3$. As is known [21], in periodogram-based methods the width of the main lobe is approximately $2\pi/P$. It follows that if a pair of angular frequencies are separated by less than $2\pi/P$, then the corresponding peaks appear as a single broader peak (smearing effect). In these circumstances the two paths cannot be resolved and large estimation errors may occur even

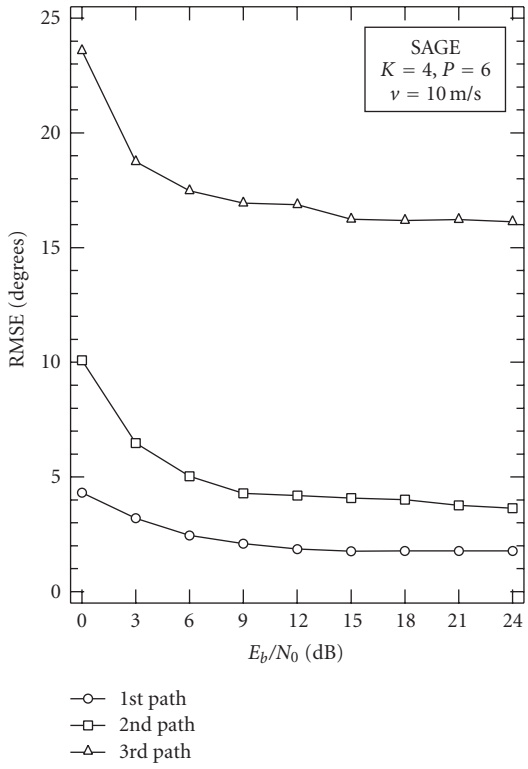

Figure 2: Performance of the SAGE estimator with $K = 4$, $P = 6$, and $v = 10$ m/s.

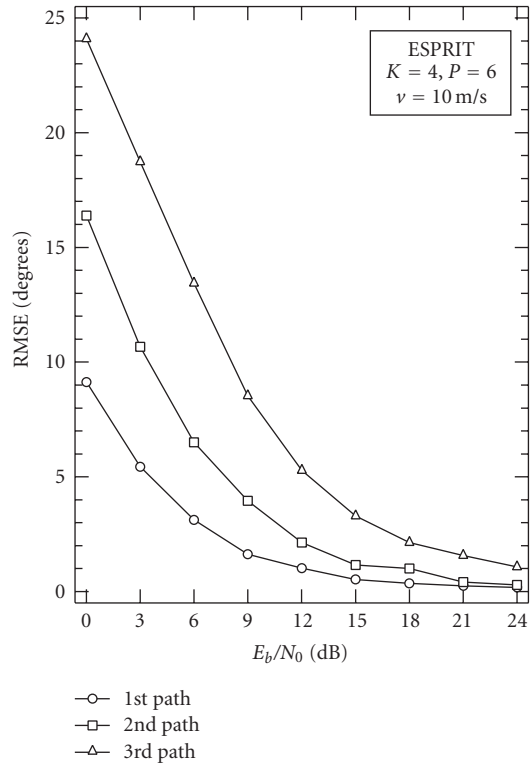

Figure 3: Performance of the ESPRIT estimator with $K = 4$, $P = 6$, and $v = 10$ m/s.

in the absence of noise. Note that in Figure 2 we have $\omega_1 = 0$, $\omega_2 = -\pi \sin 20^\circ$ and $P = 6$, so that the separation between the first and second paths is close to the resolution limit $2\pi/P$. Extensive simulations (not shown for space limitations) indicate that the floor of the SAGE estimator becomes smaller and smaller as the difference between the powers of the first and second path increases. The reason is that in these circumstances the smearing effect reduces and the parameters of the strongest path can be accurately estimated and canceled out from $\mathbf{Y}_r(i_n)$ (see (18)).

Figure 3 shows simulation results as obtained with the ESPRIT estimator in the same operating conditions of Figure 2. As we see, the RMSE curves have no floor. The reason is that ESPRIT is a *high-resolution* technique, meaning that it can resolve angular frequencies separated by less than $2\pi/P$. Comparing to Figure 2, however, it turns out that the SAGE estimator performs better than the ESPRIT at low signal-to-noise ratios (SNRs).

Figure 4 shows the performance of the SAGE scheme with $P = 6$, $v = 10$ m/s, and $K = 1$, 2, 4, or 8. In order not to overcrowd the figure, only the RMSE of the strongest path is shown. It turns out that the number of active users has little impact on the accuracy of the SAGE-based estimator. In particular, the comparison with the single-user case ($K = 1$) demonstrates the effectiveness of the proposed cancellation scheme in combating the multiple-access interference.

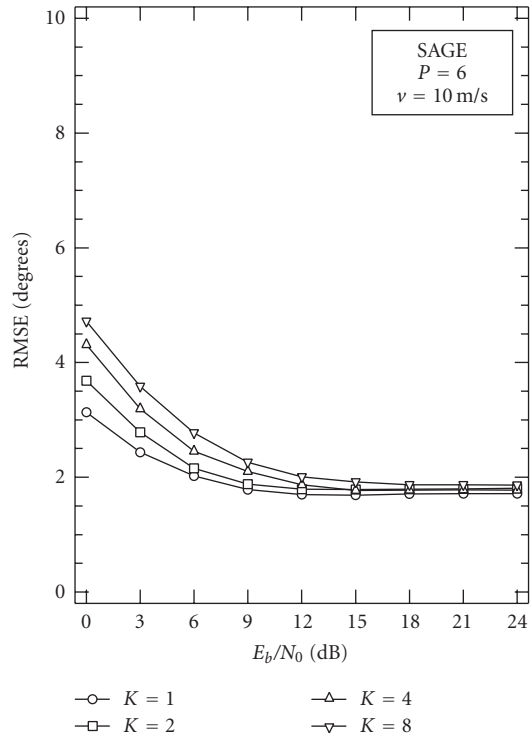

Figure 4: Performance of the SAGE estimator for $P = 6$, $v = 10$ m/s, and some values of K.

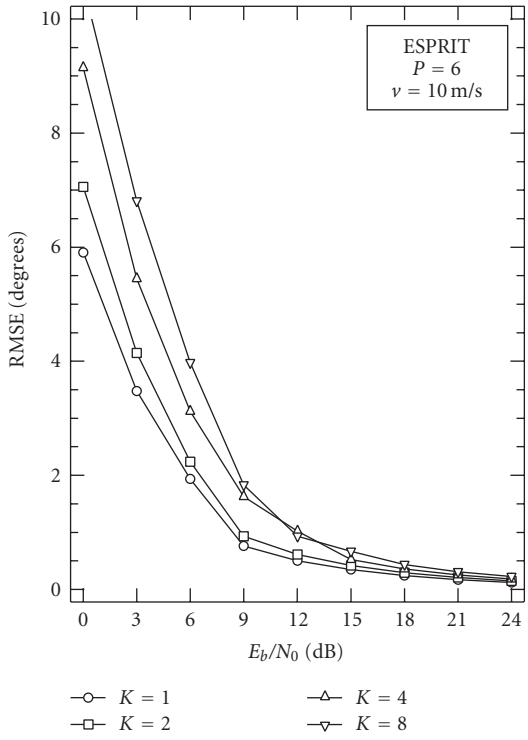

Figure 5: Performance of the ESPRIT estimator for $P = 6$, $v = 10$ m/s, and some values of K.

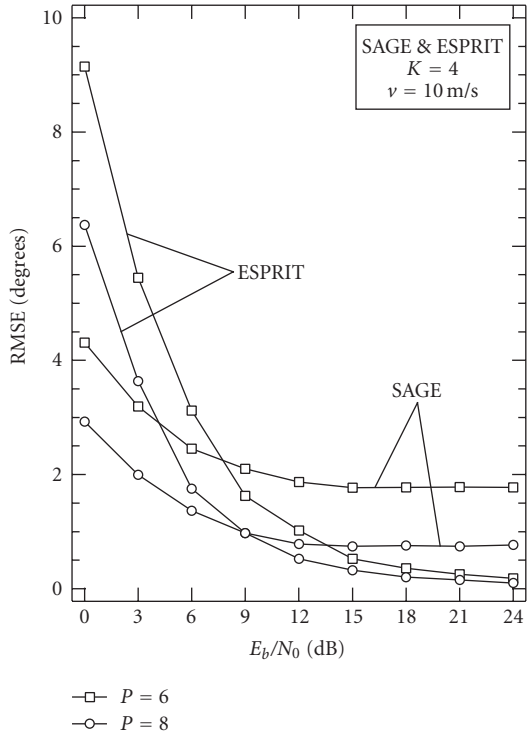

Figure 6: Comparison between the SAGE and ESPRIT estimators for $K = 4$, $v = 10$ m/s, and $P = 6$ or 8.

The same conclusions hold for the ESPRIT-based estimator, as shown by the simulation results reported in Figure 5.

The dependence of the system performance on the number of antennas is shown in Figure 6. As expected, the estimation accuracy improves as P increases. In particular, the floor in the SAGE algorithm is approximately 1.8 degrees when $P = 6$ and reduces to 0.75 degrees with $P = 8$. This can be explained bearing in mind that the resolution capability of the SAGE estimator increases with P.

Figure 7 illustrates the performance of the proposed schemes for several mobile speeds. The system is half-loaded and the number of antennas is $P = 6$. For simplicity, only the RMSE of the strongest path is shown. At first sight the results of this figure look strange in that the system performance improves as the mobile speed increases. The explanation is that the channel variations provide the system with time diversity. Actually, the DOA estimate of a weak multipath component improves if the path strength varies over the frame duration.

Figure 8 shows the complexity of the proposed DOA estimation schemes as a function of the observation length (expressed in number of data blocks per frame). The curves are computed setting $P = 6$ while the other system parameters are chosen as indicated in Section 4.1. The number of iterations with SAGE is either $N_i = 2$ or $N_i = 3$. We see that ESPRIT affords substantial computational saving with respect to the SAGE estimator. For $N_B = 128$, the latter requires approximately 2×10^5 operations while the ESPRIT allows a reduction of the system complexity by a factor 5.

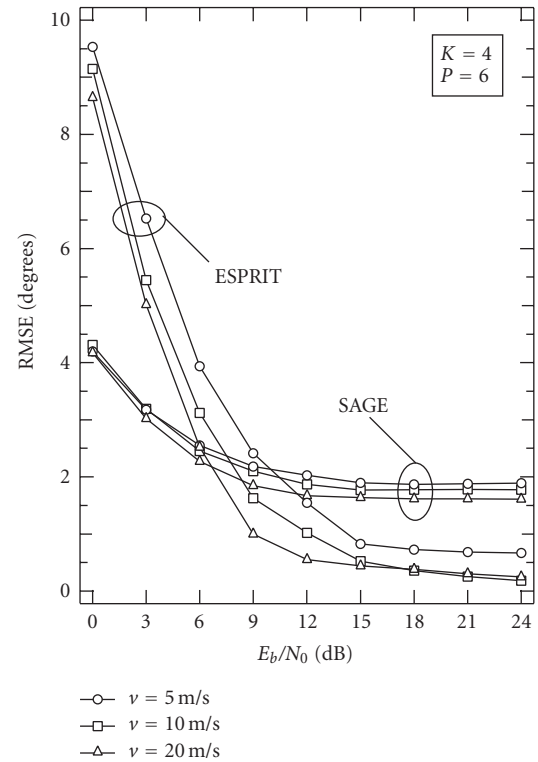

Figure 7: Performance of the proposed estimators for $K = 4$, $P = 6$, and some mobile speeds.

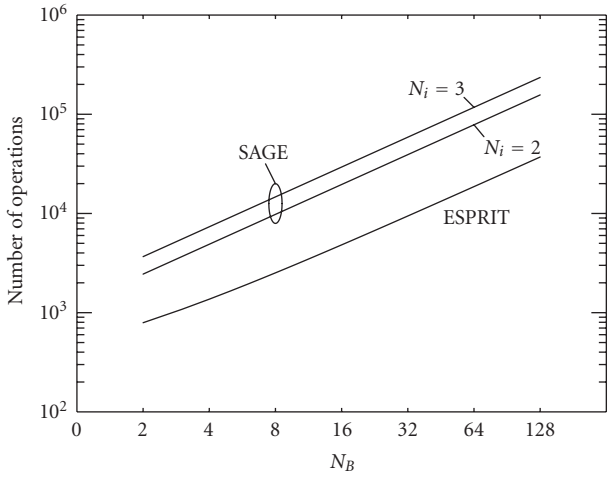

FIGURE 8: Complexity of the proposed estimators versus N_B.

5. CONCLUSIONS

We have discussed a method for estimating the DOAs of the active users in the uplink of an MC-CDMA network. Conventional DOA estimation schemes cannot be directly applied in a multiuser scenario due to the large number of parameters involved in the estimation process. Our solution exploits channel estimates and data decisions to isolate the contribution of each user from the received signal. In this way, DOA estimation is performed independently for each user employing either SAGE or ESPRIT algorithms.

Comparisons between the proposed schemes are not simple because of the different weights that may be given to the various performance indicators, that is, estimation accuracy and computational complexity. It is likely that the choice will depend on the specific application. For example, the ESPRIT is simpler and has good accuracy. On the other hand, the SAGE outperforms ESPRIT at low SNR values but has limited resolution. Using more antenna elements can alleviate this problem at the cost of an increased complexity. Computer simulations indicate that both schemes are robust against multiuser interference and channel variations.

REFERENCES

[1] L. C. Godara, "Application of antenna arrays to mobile communications—part I: performance improvement, feasibility, and system considerations," *Proceedings of the IEEE*, vol. 85, pp. 1029–1060, 1997.

[2] A. F. Naguib, A. Paulraj, and T. Kailath, "Capacity improvement with base-station antenna arrays in cellular CDMA," *IEEE Transactions on Vehicular Technology*, vol. 43, no. 3, part 2, pp. 691–698, 1994.

[3] J. C. Liberti Jr. and T. S. Rappaport, "Analytical results for capacity improvements in CDMA," *IEEE Transactions on Vehicular Technology*, vol. 43, no. 3, part 2, pp. 680–690, 1994.

[4] J. J. Caffery and G. L. Stüber, "Overview of radiolocation in CDMA cellular systems," *IEEE Communications Magazine*, vol. 36, no. 4, pp. 38–45, 1998.

[5] M. Wax and A. Leshem, "Joint estimation of time delays and directions of arrival of multiple reflections of a known signal," *IEEE Transactions on Signal Processing*, vol. 45, no. 10, pp. 2477–2484, 1997.

[6] A.-J. van der Veen, M. C. Vanderveen, and A. Paulraj, "Joint angle and delay estimation using shift-invariance techniques," *IEEE Transactions on Signal Processing*, vol. 46, no. 2, pp. 405–418, 1998.

[7] L. C. Godara, "Application of antenna arrays to mobile communications—part II: beam-forming and direction-of-arrival considerations," *Proceedings of the IEEE*, vol. 85, no. 8, pp. 1195–1245, 1997.

[8] Z. Lei and T. J. Lim, "Estimation of directions of arrival of multipath signals in CDMA systems," *IEEE Transactions on Communications*, vol. 48, no. 6, pp. 1022–1028, 2000.

[9] A. A. D'Amico, U. Mengali, and M. Morelli, "DOA and channel parameter estimation for wideband CDMA systems," *IEEE Transactions on Wireless Communications*, vol. 3, no. 6, pp. 1942–1947, 2004.

[10] K. Fazel, "Performance of CDMA/OFDM for mobile communication system," in *Proceedings of the 2nd International Conference on Universal Personal Communications (ICUPC '93)*, vol. 2, pp. 975–979, Ottawa, Ontario, Canada, October 1993.

[11] S. Hara and R. Prasad, "Overview of multicarrier CDMA," *IEEE Communications Magazine*, vol. 35, no. 12, pp. 126–133, 1997.

[12] L. Sanguinetti and M. Morelli, "Channel acquisition and tracking for MC-CDMA uplink transmissions," *IEEE Transactions on Vehicular Technology*, vol. 55, no. 3, pp. 956–967, 2006.

[13] J. A. Fessler and A. O. Hero, "Space-alternating generalized expectation-maximization algorithm," *IEEE Transactions on Signal Processing*, vol. 42, no. 10, pp. 2664–2677, 1994.

[14] R. Roy and T. Kailath, "ESPRIT-estimation of signal parameters via rotational invariance techniques," *IEEE Transactions on Acoustics, Speech, and Signal Processing*, vol. 37, no. 7, pp. 984–995, 1989.

[15] K. Deng, Q. Yin, M. Luo, and Y. Zeng, "Blind uplink channel and DOA estimator for space-time block coded MC-CDMA system with uniform linear array," in *Proceedings of the 59th IEEE Vehicular Technology Conference (VTC '04)*, vol. 1, pp. 69–73, Milan, Italy, May 2004.

[16] V. Tarokh, H. Jafarkhani, and A. R. Calderbank, "Space-time block codes from orthogonal designs," *IEEE Transactions on Information Theory*, vol. 45, no. 5, pp. 1456–1467, 1999.

[17] S. Kaiser, *Multi-carrier CDMA mobile radio systems—analysis and optimization of detection, decoding, and channel estimation*, Ph.D. thesis, VDI-Verlag, Fortschittberichte VDI, University of Kaiserslautern, Dusseldorf, Germany, 1998.

[18] M. Morelli, "Timing and frequency synchronization for the uplink of an OFDMA system," *IEEE Transactions on Communications*, vol. 52, no. 2, pp. 296–306, 2004.

[19] A. P. Dempster, N. M. Laird, and D. B. Rubin, "Maximum likelihood from incomplete data via the EM algorithm," *Journal of the Royal Statistical Society*, vol. 39, no. 1, pp. 1–38, 1977.

[20] R. Schmidt, "Multiple emitter location and signal parameter estimation," in *Proceedings of the 2nd RADC Spectrum Estimation Workshop*, pp. 243–258, Rome, NY, USA, October 1979.

[21] P. Stoica and R. Moses, *Introduction to Spectral Analysis*, Prentice-Hall, Englewood Cliffs, NJ, USA, 1997.

[22] M. Wax and T. Kailath, "Detection of signals by information theoretic criteria," *IEEE Transactions on Acoustics, Speech, and Signal Processing*, vol. 33, no. 2, pp. 387–392, 1985.